Journal of Ceramic Processing Research. Vol. 13, No. 4, pp. 480~485 (2012)

J O U R N A L O F
Ceramic Processing Research

Composition and structure of a composite spinel made from magnesia and hercynite

Guangping Liu[a], Nan Li[a,*], Wen Yan[a], Guihua Tao[b] and Yuanyuan Li[a]

[a]*The Key State Laboratory Breeding Base of Refractories and Ceramics, Wuhan University of Science and Technology, Wuhan 430081, P.R. of China*

[b]*Tongda Refractory Technologies Co. Ltd., Beijing 100084, P.R. of China*

The mineral composition, crystal structure and microstructure of a composite spinel made from magnesia and hercynite at elevated temperature were studied by X-ray diffraction (XRD), scanning electron microscopy (SEM) and energy dispersive X-ray analysis (EDAX). A composite spinel $MgFe_xAl_{2-x}O_4$ and $MgFe_2O_4$ were formed in the reaction between magnesia and hercynite, but $MgO{\cdot}Al_2O_3$ was not found. The mechanism may be described as follows: hercynite is oxidized to form γ-Al_2O_3 and γ-Fe_2O_3. MgO reacts with γ-Al_2O_3 and γ-Fe_2O_3 to form $MgO{\cdot}Al_2O_3$ and $MgO{\cdot}Fe_2O_3$, respectively. The γ-Fe_2O_3 dissolves into $MgO{\cdot}Al_2O_3$ or γ-Al_2O_3 dissolves into $MgO{\cdot}Fe_2O_3$ to form the composite spinel. The composition and crystal structure of the composite spinel depend on the sintering temperature and hercynite content in the powder mixture of magnesia and hercynite. With an increase of the sintering temperature, the solubility of Fe_2O_3 in the composite spinel decreases, resulting in an increase in 2θ, and a decrease in the lattice parameter, plane interplanar spacing and lattice distortion of the composite spinel. When the hercynite content in the mixture of magnesia and hercynite powder increases from 5 wt% to 10 wt%, the solubility of Fe_2O_3 in the composite spinel increases, resulting in a decrease in 2θ, and an increase in the lattice parameter, plane interplanar spacing and lattice distortion of the composite spinel.

Key words: Magnesia, Hercynite, Reaction, Sintering, Cement kiln.

Introduction

Magnesia chrome bricks have been widely used in cement rotary kilns for many years because of their high spalling resistance, corrosion resistance and good coating adhesion stability [1, 2]. However, Cr^{6+} brings environmental pollution. Recent years, more attention has been paid to the development of chrome-free refractories [3-14].

Magnesia hercynite refractory is an important chrome-free refractory. It has been used in cement kilns [15-20]. Hercynite ($FeAl_2O_4$) and galaxite ($MnAl_2O_4$) were called "active spinels". They were found to be the most effective to increase the flexibility of based refractories. The mechanisms of their effects have been explained as follows [20]:

1. Smaller thermal expansion of hercynite and galaxite compared to surrounding matrix, namely "thermal misfit".
2. Diffusion of Fe^{2+} ions and Mn^{2+} ions into the surrounding MgO matrix.
3. Partial diffusion of Mg^{2+} ions into the hercynite or galaxite grains and thereby Mg^{2+} ions form a local $MgO \cdot Al_2O_3$ spinel with a surplus of MgO and the Al_2O_3 from hercynite, resulting in an additional volume expansion.
4. The diffusion of Fe^{2+}, Mg^{2+} and Mn^{2+} ions proceeds during the whole operation process, such that the flexibilizing effect of its active spinels is maintained during the whole operation process.
5. Due to the diffusion processes a "crack healing process" occurs.

Five possible mechanisms mentioned above are related to the reaction between MgO and hercynite during firing. However, the composition and structure of the product in the reaction between MgO and hercynite at an elevated temperature were not investigated. In this paper, the mineral composition, crystal structure and microstructure of a composite spinel made from fused magnesia and hercynite are reported.

Experimental

Commercial fused magnesia powders and fused hercynite powders were employed as raw materials. Their chemical compositions, determined by an inductive coupled plasma emission spectrometer (ICP) (IRIS Advantage Radial, Themo Elemental Corp., USA), are shown in Table 1. The particle size distributions for the raw materials are illustrated in Fig. 1. The powder of fused magnesia has a median particle size of 33.15 μm and the powder of fused hercynite has a median particle size of 12.50 μm (by laser diffraction, Mastersizer 2000, Malvern Corp., Malvern, England).

The powder mixture A contained 10 wt% hercynite

*Corresponding author:
Tel : +86-027-68862511
Fax: +86-027-68862121
E-mail: linanref@yahoo.com.cn

Table 1. The chemical compositions of fused magnesia and fused hercynite powders (wt %)

Material	MgO	Al_2O_3	SiO_2	Fe_2O_3	CaO	K_2O	Na_2O	TiO_2
Fused magnesia	97.23	0.20	0.59	0.64	0.97	-	-	-
Fused hercynite	2.00	53.34	1.44	44.95	0.81	0.005	0.16	0.05

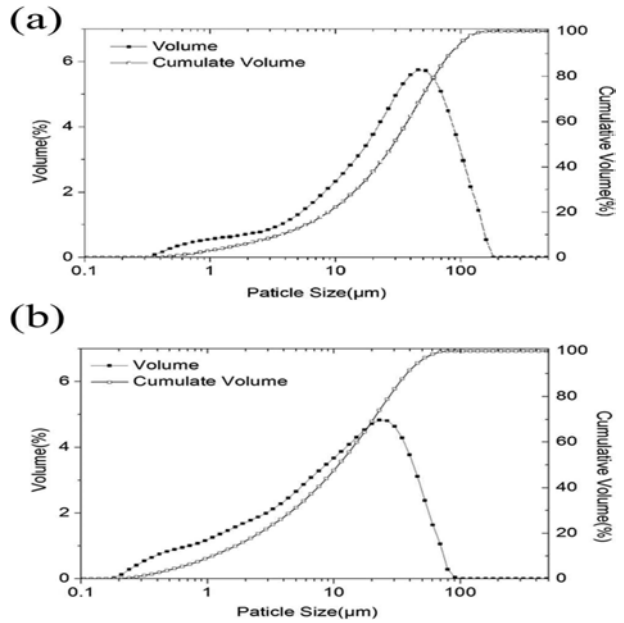

Fig. 1. Particle size distributions for (a) fused magnesia, (b) fused hercynite.

and 90 wt% fused MgO, and B contained 5 wt% hercynite and 95 wt% fused MgO. The Fe_2O_3 content in these powder mixtures was close to that in the magnesia-hercynite bricks used in industry. For comparison, sample C did not contain hercynite. The powder mixtures were pressed at 200 MPa into cylindrical samples with a diameter of 36 mm and a height of 20 mm. The green compacts were dried at 110 °C and then sintered at 1400 °C, 1500 °C and 1600 °C for 3 h in an electric furnace (Ksl1700X, Zhengzhou Experiment Instrument Co. Ltd, Zhengzhou, China).

The density and porosity of the samples were measured by the Archimedes principle in kerosene.

Phase analysis was measured by X-ray diffraction using Cu k_α radiation with a scanning speed of 2 degree per minute (X'pert PRO MPD, Philips, Eindhoven, Netherlands). The lattice parameter of the composite spinel in the samples was obtained by X'Pert Plus software. The width at half maxima (FWHM2) and $2\theta_2$ were obtained by Philips Profile Fit 1.0 software, and the crystal lattice distortion was calculated using Scherrer's law by X' Pert High Score software. The atomic ratio of Mg: Al: Fe ions of the composite spinels were calculated according to Vegard law as follows:

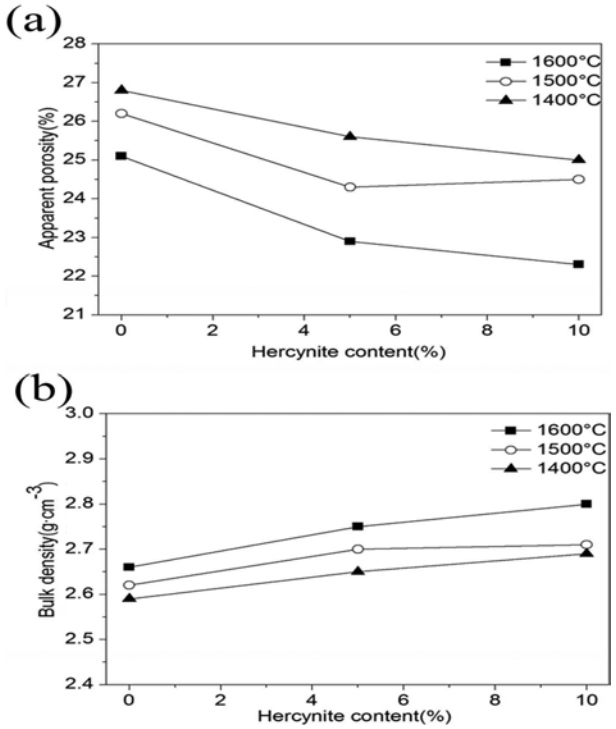

Fig. 2. Effect of the content of hercynite powder in the powder mixtures on (a) the apparent porosity and (b) bulk density of samples sintered at various temperatures for 3 h.

$$a_{ss} = a_1 x + a_2(1\text{-}x)(\text{At}\%) \quad (1)$$

where a_{ss} is the lattice parameter of the composite spinel, a_1 is the lattice parameter of component 1, x is the solubility of component 1, and a_2 is the lattice parameter of component 2.

The microstructure and composition were obtained by a scanning electron microscope with EDAX (Philips XL30 TMP, Philips, Eindhoven, Netherlands). The possible equilibrium phases were predicted by FactSage (version 6.2), and the databases of ELEM and FToxid were used.

Results and discussion

The effects of the content of the hercynite in the powder mixtures on the porosity and bulk density of samples sintered at various temperatures are illustrated in Fig. 2(a) and Fig. 2(b), respectively. It is found that with an increase of the content of hercynite, the bulk density of samples increases, while the porosity decreases. With increasing temperature, the bulk density of samples increases, and the porosity decreases.

XRD patterns of sample A, B and C sintered at 1600 °C for 3 h are shown in Fig. 3, and XRD 2θ scans of sample A and B sintered at 1600 °C for 3 h are given in Fig. 4. It is found that there is no $MgO \cdot Al_2O_3$, but a composite spinel $MgFe_{0.2}Al_{1.8}O_4$ and $MgFe_2O_4$ are found in samples A and B. $MgFe_2O_4$ spinel in the samples may come from the reaction between MgO

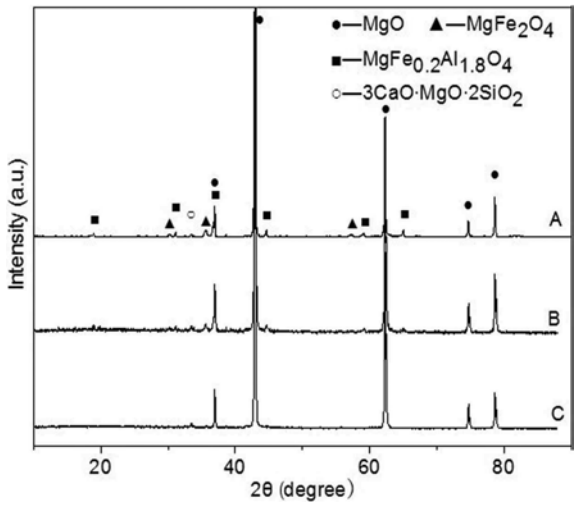

Fig. 3. XRD spectra of the sample A with the addition of 10 wt% hercynite, B 5 wt% hercynite, C without the addition of hercynite sintered at 1600 °C for 3 h.

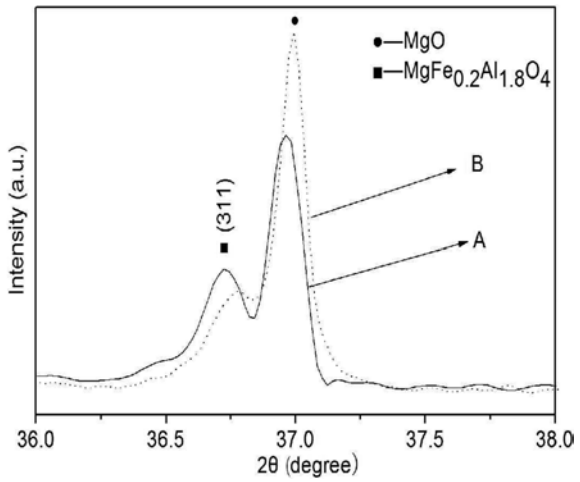

Fig. 4. XRD 2θ scans of sample A with the addition of 10 wt% hercynite, and sample B with the addition of 5 wt% hercynite sintered at 1600 °C for 3 h.

and Fe_2O_3 which is formed by the oxidation of hercynite, and minor merwinite is derived from the impurities of magnesia. The 2θ of the 311 plane of the composite spinel of sample A is 36.7313 °, and the 2θ of the 311 plane of the composite spinel of sample B is 36.7806 °.

XRD spectra and 2θ scans of sample A with the addition of 10 wt% hercynite sintered at various temperatures for 3 h are shown in Fig. 5 and Fig. 6, respectively. The mineral compositions of sample A sintered at 1400 °C, 1500 °C and 1600 °C are almost the same, but the 2θ of the composite spinel increases with an increase of the temperature, which are 36.6333 ° at 1400 °C, 36.6853 ° at 1500 °C and 36.7313 ° at 1600 °C, respectively. However, the difference of 2θ of the composite spinel between samples sintered at 1500 °C and 1600 °C is smaller than that sintered at 1400 °C and 1500 °C.

The interplanar spacing and lattice parameter of

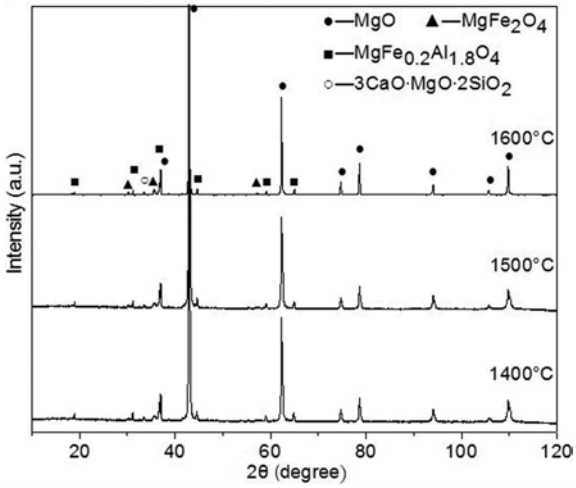

Fig. 5. XRD spectra of sample A with the addition of 10 wt% hercynite sintered at various temperatures for 3 h.

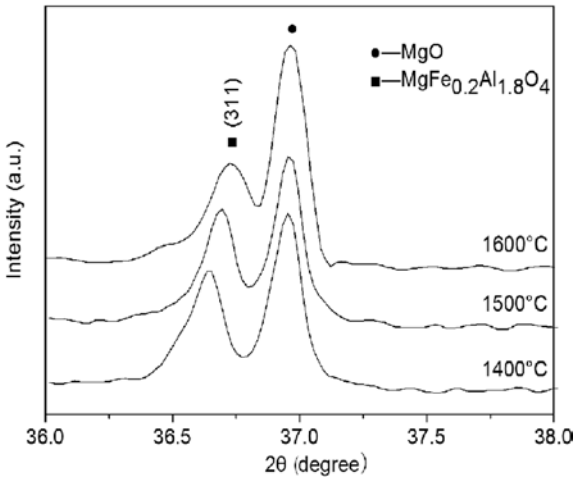

Fig. 6. XRD 2θ scans of sample A with the addition of 10 wt% hercynite sintered at various temperatures for 3 h.

Table 2. Interplanar spacings and lattice parameters of composite spinel in sample A sintered at various temperatures for 3 h and sample B sintered at 1600 °C for 3 h

Sample	311 plane interplanar spacing (Å)	2θ of 311 plane (°)	Lattice parameter a (Å)
A-1400 °C	2.45109	36.6333	8.1432
A-1500 °C	2.44773	36.6853	8.1226
A-1600 °C	2.44477	36.7313	8.1123
B-1600 °C	2.44161	36.7806	8.1039

composite spinel in sample A sintered at various temperatures for 3 h and sample B sintered at 1600 °C for 3 h calculated by X'Pert Plus software are listed in Table 2. The lattice parameter and 311 plane interplanar spacing of the composite spinel in sample A decrease with an increase of the temperature. When the hercynite content in the mixture of magnesia and hercynite powder was increased from 5 wt% to 10 wt%, 2θ of the composite spinel decreased, while the lattice parameter

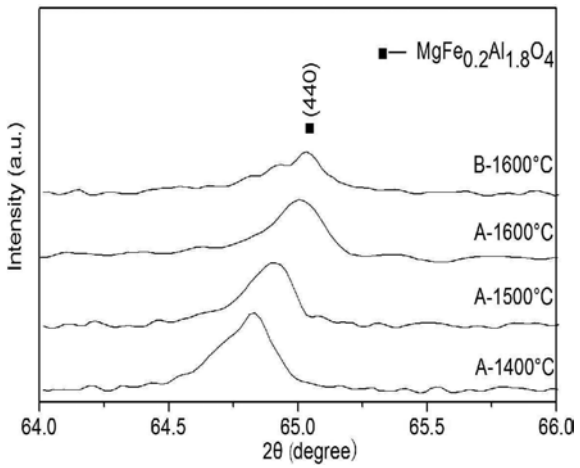

Fig. 7. XRD $2\theta_2$ scan spectra of sample A with the addition of 10 wt% hercynite sintered at various temperatures for 3 h and sample B with the addition of 5 wt% hercynite sintered at 1600 °C for 3 h.

Table 3. FWHM2, $2\theta_2$, and crystal lattice distortions of composite spinel in sample A sintered at various temperatures for 3 h and sample B sintered at 1600 °C for 3 h

Sample	FWHM2 (°)	$2\theta_2$ (°)	Crystal lattice distortion (%)
A-1400°C	0.2429	64.8065	0.152
A-1500°C	0.2097	64.8906	0.127
A-1600°C	0.2071	64.9991	0.124
B-1600°C	0.1781	65.0389	0.101

and plane interplanar spacing of the composite spinel increased.

The $2\theta_2$ scans of the samples sintered at various temperatures for 3 h are shown in Fig. 7, and FWHM2 and crystal lattice distortion of composite spinel in sample A sintered at various temperatures for 3 h and sample B sintered at 1600 °C for 3 h are listed in Table 3. When the temperature was increased from 1400 °C to 1500 °C, the crystal lattice distortion decreased obviously, but when the temperature was raised from 1500 °C to 1600 °C, the crystal lattice distortion changed slightly. The lattice distortion of sample B sintered at 1600 °C is less than that of sample A sintered at 1600 °C, because the former has less hercynite content than the latter.

SEM micrographs of the samples sintered at various temperatures for 3 h are shown in Fig. 8. EDAX analyses results are listed in Table 4. According to the results, the possible phase compositions of sample A sintered at various temperatures are a composite spinel, $MgO\text{-}Fe_2O_3$ solid solution, a small amount of a compound in the $CaO\text{-}MgO\text{-}SiO_2$ system and a low-melting phase.

Based on the EDAX results in Table 4, the average atomic ratio of Mg: Al: Fe in the composite spinel of sample A sintered at various temperatures for 3 h was obtained, as shown in Table 5. The average atomic ratios of Mg: Al: Fe in the composite spinel of sample A sintered at 1400 °C, 1500 °C and 1600 °C are 1:1.79:0.39, 1:1.84:0.28 and 1:1.90:0.20, respectively.

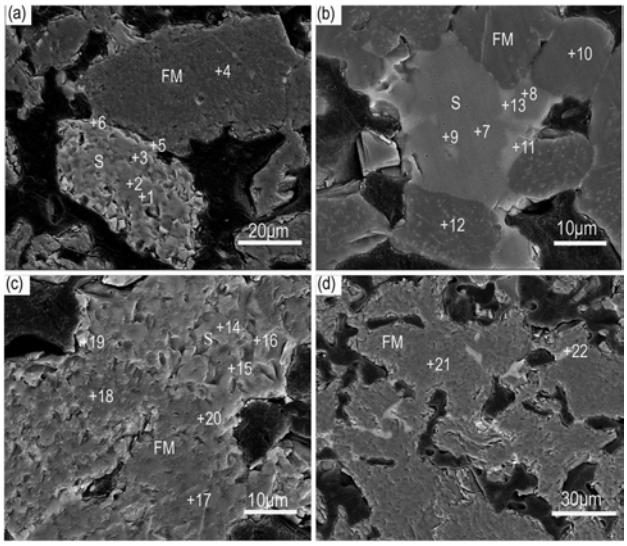

Fig. 8. SEM micrographs of the samples with the addition of 10 wt% of hercynite sintered for 3 h at (a) 1400 °C, (b) 1500 °C, (c) 1600 °C and (d) without the addition of hercynite sintered at 1600 °C for 3 h. FM, Fused magnesia, S, Composite spinel. Table 6 lists EDAX results for points in Fig. 8.

Table 4. EDAX analyses results in atomic (%) for points in Fig. 8

at. %	O	Mg	Al	Si	Ca	Fe	Possible phases
1	44.60	18.18	29.78			7.45	Composite spinel
2	48.71	16.11	28.74			6.44	
3	50.02	14.83	29.08		0.88	5.19	
7	46.69	17.31	30.97			5.04	
8	48.41	16.69	30.85			4.05	
9	50.23	15.67	29.40			4.70	
14	53.47	15.54	27.78			3.21	
15	51.24	15.06	30.46			3.24	
16	56.69	14.07	26.82			2.42	
4	40.89	57.51				1.60	$MgO\text{-}Fe_2O_3$ solid solution
10	40.55	57.63				1.82	
12	39.43	58.54				2.03	
17	42.72	55.36				1.92	
18	42.94	54.38				2.68	
20	46.07	52.97				0.96	
21	42.91	57.09					Periclase
5	57.17	17.29		10.55	14.99		Compound in $CaO\text{-}MgO\text{-}SiO_2$
11	58.65	16.41		10.46	14.48		
22	56.25	7.03		15.07	21.66		
6	56.07	12.60	18.01	3.84	6.16	3.33	Low-melting phase
13	57.62	9.33	6.39	10.82	14.42	1.42	
19	58.65	9.87	8.41	9.16	12.16	1.74	

Table 5. Average atomic ratios of Mg : Al : Fe in the composite spinel in sample A sintered at various temperatures for 3 h (calculated from the EDAX results)

Element	1400 °C	1500 °C	1600 °C
(Fe + Al)/Mg	2.18	2.12	2.10
Mg:Al:Fe	1:1.79:0.39	1:1.84:0.28	1:1.90:0.20

Table 6. Atomic ratios of Mg : Al : Fe in composite spinel in sample A sintered at various temperatures for 3 h (calculated by Vegard law)

temperature	spinel formed from $MgFe_2O_4$ and $MgAl_2O_4$		spinel formed from $FeAl_2O_4$ and $MgAl_2O_4$	
	$MgFe_2O_4$: $MgAl_2O_4$	Mg:Al:Fe	$FeAl_2O_4$: $MgAl_2O_4$	Mg:Al:Fe
1400 °C	19.76:80.24	1:1.60:0.40	85.49:14.51	1:13.78:5.89
1500 °C	12.98:87.02	1:1.74:0.26	56.19:43.81	1:4.57:1.28
1600 °C	9.60:90.40	1:1.81:0.19	35.14:64.86	1:3.08:0.54

As the temperature increases, the Fe content in composite spinel decreases. The composite spinel may be described as $MgFe_xAl_{2-x}O_4$, because its composite changes with temperature and hercynite content in the powder mixture.

Lavina et al. reported that hercynite was oxidized in an air atmosphere at 600 °C to form γ-Al_2O_3 and γ-Fe_2O_3, as [21]:

$$FeAl_2O_4 + \frac{1}{4}O_2 = \frac{1}{2}\ \gamma\text{-}Fe_2O_3 + \gamma\text{-}Al_2O_3 \qquad (2)$$

A result of the study by thermochemical software FactSage 6.2 is shown in Fig. 9, using starting materials of MgO (90 wt%), $FeAl_2O_4$ (10 wt%) and excess oxygen. It is found that $FeAl_2O_4$ disappears and a composite spinel (spinel#1) appears. The γ-Al_2O_3 formed reacts with MgO to form $MgAl_2O_4$ rapidly. γ-Al_2O_3 was found to be beneficial to synthesize a spinel because it had a crystal structure similar to that of a spinel [22]. A part of γ-Fe_2O_3 reacts with MgO to form $MgFe_2O_4$, and a part of γ-Fe_2O_3 dissolves into $MgAl_2O_4$ to form a composite spinel. In order to understand the mechanism of formation of the composite spinel, we suppose that the composite spinel is formed by interdiffusion between $MgAl_2O_4$ (JCPDS: 21-1152, a = 8.0831 Å) and $MgFe_2O_4$ (JCPDS: 36-0398, a = 8.3873 Å), or between $MgAl_2O_4$ and $FeAl_2O_4$ (JCPDS: 34-0192, a = 8.1534 Å). The atomic ratio of Mg: Al: Fe in the composite spinels in sample A sintered at various temperatures for 3 h is given in Table 6. They were calculated based on Vegard law (Eq. 1) and lattice parameters obtained from XRD. Comparing Table 5 and Table 6, it is found that the average atomic ratio of Mg: Al: Fe obtained from EDAX is very close to the atomic ratio of Mg: Al: Fe obtained from XRD of the composite spinel which is formed from interdiffusion by $MgAl_2O_4$ and $MgFe_2O_4$. The mechanism of formation of the composite spinel

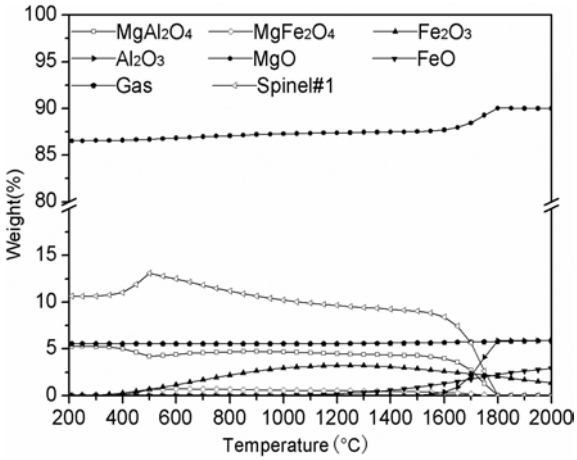

Fig. 9. Species predicted of MgO (90 wt%), $FeAl_2O_4$ (10 wt%) and excess oxygen as a function of temperature.

may be described as follows:

$FeAl_2O_4$ is oxidized to form γ-Al_2O_3 and γ-Fe_2O_3. γ-Al_2O_3 and γ-Fe_2O_3 react with MgO to form $MgAl_2O_4$ and $MgFe_2O_4$, respectively. Some of the γ-Fe_2O_3 dissolves into $MgAl_2O_4$ to form a composite spinel, at the same time γ-Al_2O_3 may dissolve into $MgFe_2O_4$ to form a composite spinel. If the particles of $MgAl_2O_4$ and $MgFe_2O_4$ touch each other, a composite spinel may form by interdiffusion between $MgAl_2O_4$ and $MgFe_2O_4$. Because the Fe content in the composite spinel is the least, it may be considered that the composite spinel is a solid solution of a spinel by solution of Fe_2O_3 into $MgAl_2O_4$. With an increase of the sintering temperature, the solubility of Fe_2O_3 decreases, resulting in an increase in 2θ, and a decrease in the lattice parameter, plane interplanar spacing and lattice distortion of the composite spinel. When the sintering temperature increases from 1400 °C to 1500 °C, the reduction of Fe content in the composite spinel is more than that when the sintering temperature increases from 1500 °C to 1600 °C. The reductions of lattice parameter, plane interplanar spacing and lattice distortion of the former are also more than those of the latter. Because the hercynite content in sample A is larger than that in sample B, the solubility of Fe_2O_3 in the composite spinel in sample A sintered at 1600 °C is larger than that in sample B, resulting in the lattice parameter, plane interplanar spacing, FWHM2 and lattice distortion of the composite spinel in sample A are larger than those of sample B, and 2θ is less than the 2θ of sample B. The larger lattice distortion in sample A improves sintering, resulting in a decrease of the apparent porosity. At the same time, a greater Fe_2O_3 content may increase the liquid content in sample A at 1600 °C, which is another reason to decrease the apparent porosity of sample A.

Conclusions

In the product formed in the reaction between MgO and hercynite at elevated temperature, there is no

$MgO \cdot Al_2O_3$, but a composite spinel $MgFe_xAl_{2-x}O_4$ and $MgFe_2O_4$ are found. $FeAl_2O_4$ is oxidized to form γ-Al_2O_3 and γ-Fe_2O_3 firstly. MgO reacts with γ-Al_2O_3 and γ-Fe_2O_3 to form $MgO \cdot Al_2O_3$ and $MgO \cdot Fe_2O_3$. γ-Fe_2O_3 dissolves into $MgO \cdot Al_2O_3$ or γ-Al_2O_3 dissolves into $MgO \cdot Fe_2O_3$ to form a composite spinel. The composition and crystal structure of the composite spinel depend on the sintering temperature and hercynite content in the powder mixture of magnesia and hercynite. With an increase of sintering temperature, the solubility of Fe_2O_3 decreases, resulting in an increase in 2θ, and a decrease in the lattice parameter, plane interplanar spacing and lattice distortion of the composite spinel. When the sintering temperature increases from 1400 °C to 1500 °C, the effects of temperature on the structure and composition of composite spinel are stronger. The solubility of Fe_2O_3 in the composite spinel in the sample with a higher hercynite content is higher than that with a lower hercynite content, resulting in a decrease in 2θ, and an increase in lattice parameter, plane interplanar spacing and lattice distortion of the composite spinel. With an increase in the hercynite content and temperature, the bulk density of the compacts increases, while the porosity decreases.

Acknowledgements

We wish to express our thanks to the Tongda Refractory Technologies Co., Ltd for financially supporting this work.

References

1. P. Bartha and H. J. Klischat, CN-Refractories 6 [3] (1999) 31-38.
2. W.E. Lee and R.E. Moore, J. Am. Ceram. Soc. 81 [6] (1998) 1385-1410.
3. H. Komatsu, M. Arai, and S. Ukawa, Taikabutsu Overseas 19 [4] (1999) 3-9.
4. J. Nievoll and B. Buchberger, Veitsch-Rades Rundschau 1 (1999) 57-64.
5. M. Arai and U. Shigeru, in Proceeding of Unified International Technical Congress on Refractories, Osaka, Japan, 2003, p. 43-46.
6. M. Ohno, K. Tokunaga, Y. Tsuchiya, Y. Mizuno, and H. Kozuka, in Proceeding of Unified International Technical Congress on Refractories, Osaka, Japan, 2003, p. 27-30.
7. B. Mishra, in Proceeding of Unified International Technical Congress on Refractories, Salvador, Brazil, 2009.
8. H. Kozuka, Y. Kaita, Y. Tuchiya, T. Honda, and S. Ohta, in Proceeding of Unified International Technical Congress on Refractories, Brasil, Sao Paulo, 1993, p. 1027-1037.
9. H. Kozuka, Y. Kajita, Y. Tuchiya, T. Honda, and S. Ohta, in Proceeding of Unified International Technical Congress on Refractories, Kyoto, Japan,1995, p. 256-263.
10. S. Serena, M.A. Sainz, and A. Caballero, J. Eur. Ceram. Soc. 24 [8] (2004) 2399-2406.
11. S. Serena, M.A. Sainz, and A. Caballero, J. Eur. Ceram. Soc. 29 [11] (2009) 2199-2209.
12. J.L.R. Galicia, A.H.D. Aza, J.C.R. Angeles, and P. Pena, J. Eur. Ceram. Soc. 27 [1] (2007) 79-89.
13. E. Rodriguez, GA. Castillo, and A.M. Guzman, in Proceeding of Unified International Technical Congress on Refractories, Salvador, Brazil, 2009.
14. J. Szczerba, Ceram. Int. 36 [6] (2010) 1877-1885.
15. G. Buchebner, H. Harmuth, and T. Mdami, in Proceeding of Unified International Technical Congress on Refractories, Berlin, Germany, 1999, p. 201-203.
16. N. Josef, Z.Q. Guo, and S. Shi, RHI Bulletin 3 (2006) 15-17.
17. H.Z. Gu, H.Z. Wang, and B. Yang, in Proceeding of Unified International Technical Congress on Refractories, Salvador, Brazil, 2009.
18. J.E. Contreras, GA. Castillo, E.A. Rodriguez, T.K. Das, and A.M. Guzman, Mater. Charact. 54 [4] (2005) 354-359.
19. J.H. Chen, L.Y. Yu, J.L Sun, Y. Li, and W.D. Xue, J. Eur. Ceram. Soc. 31 [3] (2011) 259-263.
20. G. Martin, M. Christian, and W. Andreas, RHI Bulletin 1 (2003) 25-28.
21. B. Lavina, F. Princivalle, and A.D. Giusta, Phys. Chem. Miner. 32 [2] (2005) 83-88.
22. Z.H. Zhang and N. Li, Ceram. Int. 31 [4] (2005) 583-589.